Spectrum assignment for industrial radio cells based on selective subgraph constructions

Gilberto Berardinelli, Ramoni Adeogun
Department of Electronic Systems, Aalborg University, Denmark
E-mail:{gb, ra}@es.aau.dk

***Abstract*—Dense industrial wireless cells have to ensure minimum survival rates such that the mission critical functionalities can at least be supported regardless of the deployment and interference conditions. In this paper, we propose a novel spectrum allocation mechanism meant to efficiently support minimum survival rates but without compromising the average network performance. The presented approach is based on a two-phase graph construction and coloring, where cells that are still experiencing mutual interference upon a first frequency allocation are further orthogonalized. Simulation results show that our solution can lead to an increase of up to $\sim$250% of the survival rates with negligible impact on the average network throughput.**

***Index Terms*—Industrial radio cells, spectrum allocation, interference management, mission critical communication**

I. Introduction

Upcoming Industry 4.0 use cases can highly benefit from wireless technologies for overcoming the burden of cabling, its inherent lack of flexibility, as well as its associated installation and maintenance costs. Recent visions on industrial wireless deployments feature short range low power radio cells to be installed in industrial production modules and static or mobile robots [1]. Part of the industrial cells applications are mission critical and are required to run at every condition at the expected quality level, while others may tolerate degradation and even partial interruptions. The former are typically associated to closed loop control featuring periodic deterministic traffic and low guaranteed bit rates, while the latter can be associated, for example, to monitoring video feeds with scalable quality. In order to support at least the mission critical services, minimum *survival* data rates should then be guaranteed at each cell.

The potential high density of industrial radio cells raises the issue of ensuring a proper allocation of the radio resources such that at least the performance requirements for mission critical services can be achieved in spite of potentially harsh mutual interference. The problem of interference management in dense deployments has been widely discussed in the last decades and is historically handled via static or dynamic frequency reuse, where the available bandwidth is divided in a number of subbands to be allocated at each cell such that mutual interference is minimized [2]. Other approaches, based on time domain resource allocation or selective muting, appears unsuited for industrial cells as they impact the latency of cells supporting periodic deterministic traffic [1].

A well known approach for interference management, adopted since the early days of cellular networks [3], is to represent the network as a conflict graph where the vertex are the cells, and the edges connect the cells experiencing significant interference. Graph coloring aims then at assigning at each vertex a color, representing specific resources (e.g., a frequency subband), such that no edges with the same color exist [4]. This way, the cells are allocated over resources where low mutual interference levels are experienced. An exhaustive survey of graph coloring approaches applied to cellular network is presented in [5]. Among the relevant recent works, graph coloring is applied in [6] for improving downlink performance of dense femtocells and their coexistence with a macro network operating in the same spectrum, while distributed solutions are presented in [7], [8]. Coloring graphs with a large number of colors translates to the usage of small subbands and may preserve minimum rates. However, it can severely impact the average cell throughput as every cell ends up operating over a subband of limited size even when its perceived interference levels are low.

In this paper, we propose a novel centralized spectrum assignment solution for dense industrial cells based on a selective subgraph construction. In a first phase, a conflict graph is built upon the interference relationship among the cells. In a second stage, eventual subgraphs are constructed in case cells allocated in the same subbands are still unable to achieve a sufficient data rate. Our goal is to ensure sufficient minimum survival rates but without severely compromising the average cell throughput. The presented solution is inspired to the known concept of fractional frequency reuse in cellular networks, where cell area is partitioned into regions with different frequency reuse factors [9]; however, in our concept we are targeting small industrial cells with very limited radius, and different subband sizes are therefore applied on a cell basis. It is worth mentioning that our contribution does not lie in novel graph coloring methods, but rather on the graph identification and construction approaches for interference mitigation.

The paper is structured as follows. Section II introduces the general scenario, as well as the baseline approach for graph construction. Our proposed selective subgraph construction procedure is presented in section III, along with an illustrative example. Numerical results are reported in Section IV. Finally, Section V concludes the paper and states the future work.

II. Setting up the scene

We consider N radio cells consisting of an access point (AP) and $\mathrm{n_d}$ devices deployed in a factory hall. Each cell has a radius r, and devices are randomly distributed in the cell area. A centralized network controller manages a band of size W to be shared among the cells. The main objective is to assign spectrum such that of a minimum survival rate for supporting at least the very critical operations is guaranteed at each cell regardless of the specific deployment.

Without losing in generality, we assume that cells operate in time division duplex (TDD) mode, where uplink and downlink transmission are multiplexed in time. Also, we assume that transmit power is the same on uplink and downlink. These are reasonable assumptions for short range low power cells [1]. The cells are synchronized at frame level, but not in the TDD switching point. As a consequence, cross-link interference (e.g. uplink-to-downlink or downlink-to-uplink) may appear besides same link interference. We assume that each cell is able to estimate the interference coming from the other cells. In a practical implementation, this can be obtained by introducing a common control channel where each cell (in turn, devices and AP) is broadcasting a beacon in a round robin fashion, while other cells are listening. A cell can eventually aggregate measurements performed by devices and by the AP itself, and report it to the central controller. This way, the central controller is able to build a deployment interference matrix $\mathbf{I}$, of dimension $\mathrm{N} \times \mathrm{N}$, whose generic element $\mathbf{I}(p,q)$, $p = 1,\ldots,\mathrm{N}$, $q = 1,\cdots,\mathrm{N}$, represents the interference measured at cell p from cell q. By design, $\mathbf{I}(p,p) = 0$ for $p = 1,\cdots,\mathrm{N}$.

A typical subband assignment procedure based on a conflict graph construction is then performed. The central controller defines a graph $\mathrm{G} = \{\mathrm{V},\mathrm{E}\}$ where the vertexes V represent the cells and E are the edges. The graph can be constructed with different approaches. In this paper, we adopt a bonding criterion with respect to the M strongest neighbors. By denoting as $\mathrm{T_{M,u}}$ the set of M strongest interfering cells measured at cell u, an edge in the graph between vertex u and vertex v exists if v belongs to that set, i.e. $(u,v) \in \mathrm{E}$ if $v \in \mathrm{T_{M,u}}$.

A vertex coloring process is then applied by assigning at each vertex a color such that none of the vertexes connected by an edge have the same color. Since an optimal coloring scheme based on brute-force search or dynamic programming is impractical for sufficiently large graphs, heuristics such as greedy-coloring are usually adopted [10]. In case the vertices are ordered according to the number of incident edges, greedy colorings can be completed in linear time. It is know that greedy coloring does not guarantee that the minimum number of colors is used. However, it can be stated that $\mathrm{N_C} \leq \Delta + 1$, where $\mathrm{N_C}$ is the number of assigned colors and Δ denotes the maximum number of edges incident to a vertex in the graph [10].

The central controller divides then the band W in $\mathrm{N_C}$ subbands of size $\frac{\mathrm{W}}{\mathrm{N_C}}$, such that there is a one-to-one mapping between the assigned color and the selected subband. Note that, in practical applications, an improper graph coloring might be used in case the number of channels to be assigned is imposed beforehand [11]. This first phase graph construction, that follows a known approach as used in previous work (e.g., [6], [12]), will be considered as a benchmark in the numerical analysis for evaluating the benefits of a second phase selective subgraph construction presented next.

III. Subgraph construction procedure

The main idea of the proposed subgraph construction procedure is to further fraction the subbands assigned in the initial phase for those cells that are still expected to experience unsatisfactory conditions, while letting unaltered the allocation for the other cells, such that they can achieve higher rates. This is done by first identifying the interference-bonded cells in each of the subbands, build the corresponding interference submatrix and the respective subgraphs, and color the subgraphs again. Such steps are illustrated in the following.

1) Cell subset selection: Let us denote with $\mathrm{C_z}$ the set of cells assigned to color z, for $z = 1,\cdots,\mathrm{N_C}$. We define the subsets $\mathrm{L_z}$ and $\mathrm{D_z}$ as follows:

- the subset $\mathrm{L_z}$ includes all the cells in $\mathrm{C_z}$ with limited estimated data rate, i.e. $p \in \mathrm{L_z}$ if $\mathrm{R\,(p)} < \mathrm{R_{th}}$, $\forall p \in \mathrm{C_z}$, where $\mathrm{R\,(p)}$ denotes an estimate of the data rate for cell p assuming the band allocation in the first phase, and $\mathrm{R_{th}}$ is a predefined data rate threshold;
- the subset $\mathrm{D_z}$ includes the strongest interferers to the nodes in $\mathrm{L_z}$, such as $q \in \mathrm{D_z}$ if $q = \mathrm{argmax_m}\mathbf{I}(\mathrm{p,m})$, $\forall p \in \mathrm{L_z}$, $\forall m \in \mathrm{C_z}$.

The relevant subset of residual cells with strong bond in the set $\mathrm{C_z}$, for $z = 1,\cdots,\mathrm{N_C}$, is then given by $\tilde{\mathrm{C}}_\mathrm{z} = \mathrm{L_z} \cup \mathrm{D_z}$.

2) Inteference submatrix calculation: Such subset $\tilde{\mathrm{C}}_\mathrm{z} \subseteq \mathrm{C_z}$ is then used for generating a corresponding interference submatrix. The interference submatrix $\tilde{\mathbf{I}}_z$ is obtained by selecting the elements in $\mathbf{I}$ corresponding to the cells in $\tilde{\mathrm{C}}_\mathrm{z}$. By denoting as $j(p)$ the index of the set $\tilde{\mathrm{C}}_\mathrm{z}$ corresponding to cell p, the generic element of the submatrix $\tilde{\mathbf{I}}_z$ is given by $\tilde{\mathbf{I}}_z(j(p),j(q)) = \mathbf{I}(p,q)$, $\forall p,q \in \tilde{\mathrm{C}}_\mathrm{z}$. Such submatrix has dimension $\left|\tilde{\mathrm{C}}_\mathrm{z}\right| \times \left|\tilde{\mathrm{C}}_\mathrm{z}\right|$, where $\left|\tilde{\mathrm{C}}_\mathrm{z}\right|$ denotes the cardinality of the subset $\tilde{\mathrm{C}}_\mathrm{z}$.

3) Subgraph construction: Subgraphs for each subset can be constructed again according to a strong neighbor criterion. As the cardinality of a subset can be very small in this second phase, the number of neighbors is defined as $\mathrm{M_z} = \min(\left|\tilde{\mathrm{C}}_\mathrm{z}\right| - 1, \mathrm{M}')$, where M' is a predefined maximum number of neighbor for the subgraph construction. A new graph $\mathrm{G_z} = \{\mathrm{V_z},\mathrm{E_z}\}$ for subset $\tilde{\mathrm{C}}_\mathrm{z}$ is then defined. By denoting as $\mathrm{T_{z,M_z,u}}$ the set of the $\mathrm{M_z}$ strongest interferers to the cell $u \in \tilde{\mathrm{C}}_\mathrm{z}$, an edge in the graph between vertex u and vertex v exists if $v \in \mathrm{T_{z,M_z,u}}$, i.e. $(u,v) \in \mathrm{E_z}$ if $v \in \mathrm{T_{z,M_z,u}}$.

Such graph is also colored. As a result, each cell will be associated a color such that none of the $\mathrm{M_z}$ strongest interferers have the same color. The controller will be further dividing subband z in $\mathrm{N_{C,z}}$ chunks of size $\frac{\mathrm{W}}{\mathrm{N_C N_{C,z}}}$, where $\mathrm{N_{c,z}}$ is the resulting number of colors in $\tilde{\mathrm{C}}_\mathrm{z}$, and assign each cell

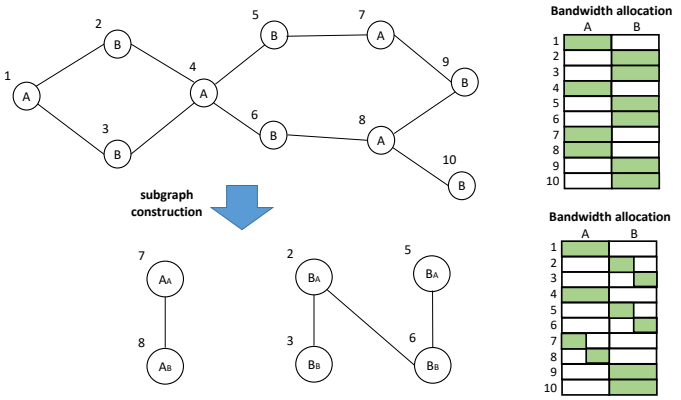

Fig. 1. Example of of selective subgraphs construction and bandwidth allocation.

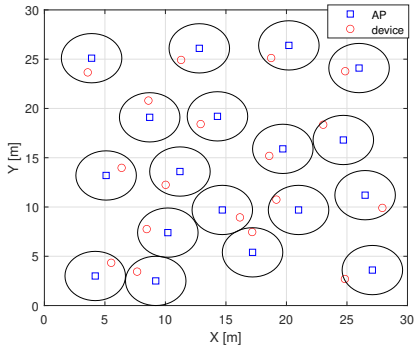

Fig. 2. Example of network deployment.

to the chunks according to the color assigned at the second phase. Note that, in case $\tilde{\mathrm{C}}_{\mathrm{z}} = \emptyset$, the second phase coloring for group C_{z} does not take place, as cells associated to the same subband after the first phase are deemed not to generate significant mutual harm. In case greedy coloring with vertex ordering is used in both phases, the presented solution has a linear complexity.

A. Illustrative example

An illustrative example of subgraph construction and coloring is depicted in Figure 1. Each cell is associated to a node in the graph, and denoted with numerical indexes $1, 2, \cdots, 10$. In the first stage, the graph is built assuming $\mathrm{M} = 1$, i.e. each node has an edge with the strongest neighbor only. We assume the graph to be 2-colorable, i.e. $\mathrm{N_C} = 2$, and the resulting colors are denoted with A, B. Each color is associated to a subband, as shown in the top right side of the figure. The two sets are $\mathrm{C_A} = \{1, 4, 7, 8\}$, and $\mathrm{C_B} = \{2, 3, 5, 6, 9, 10\}$.

In the next phase, the nodes that are still generating mutual harm in the same subband are identified according to the criterion presented earlier. For subband A, the subset $\tilde{\mathrm{C}}_{\mathrm{A}} = \{7, 8\}$ is identified, while for subband B, the subset $\tilde{\mathrm{C}}_{\mathrm{B}} = \{2, 3, 5, 6\}$ is identified. Subgraphs are then built for each of these groups, assuming $\mathrm{M}' = 1$. These subgraphs are also assumed to be 2-colorable, and the color associated at each node is indicated by a subscript, i.e. $\mathrm{A_B}$ denotes allocation of a second phase color B to a cell whose first phase allocation was color A. Such new colors are also associated to a portion of the previous subband. As a consequence, cells that are still generating mutual performance harm in spite of the first allocation, are further orthogonalized; they will then operating over a smaller subband, further reducing their maximum achievable rate, but avoiding significant mutual interference.

IV. Numerical results

The performance of the proposed selective subgraph construction procedure for spectrum allocation is analyzed via MATLAB simulations. We consider $N = 18$ cells deployed in a 30×30 m^2 factory hall. For simplicity, but without losing in generality, we assume that each cell serves only $\mathrm{n_d} = 1$ device. Each cell has a radius of $\mathrm{r} = 2.5$ m, with the AP located at the cell center and the device randomly deployed in the cell area with a minimum distance from the AP of 1 m. A possible network deployment is shown in Figure 2.

The radio propagation parameters are set according to the 3GPP non-line-of-sight industrial channel model for sparse clutter [13], with a shadowing fading standard deviation of 5.7 dB, and a 3.5 GHz carrier frequency. Note that the presence of shadow fading leads to scenario where the strongest interference contribution may not come from the geographically closer cells.

We consider static deployments. In deployments characterized by varying channel condition or mobile appearing/disappearing cells, the spectrum assignment procedure must be repeated frequently enough for copying with the varying interference conditions. A performance analysis with time varying deployments is left for future work.

The network controller takes care of allocating a band W= 100 MHz to the cells. While most of the studies for best effort cellular communication analyze cell edge performance at the 5-10%-ile of the data rate distribution, given our need of supporting mission critical services we analyze the survival rates at the significantly stricter 0.001%-ile.

The analysis is here focused on the downlink only, as this represents in our deployment the most challenging case for the support of survival rates. This is because the potential cross-link uplink-to-downlink interference can be more detrimental than the downlink-to-uplink interference, as devices belonging to different cells may be located at a close distance (as also visible for some of the cells in Figure 2), while the APs are always located at the center of the respective cells.

Both AP and device are transmitting at a fixed power $\mathrm{P_t} = 0$ dBm regardless of the allocated subband size. This means, the power spectral density increases in proportion to the reduction of subband allocation. Both the estimated data rate threshold $\mathrm{R_{th}}$ triggering subgraph construction, and the actual data rate once allocation is performed, are calculated as $\mathrm{B} \cdot \log_2\left(1 + \frac{\mathrm{P_r}}{\mathrm{Z} + \sigma^2 \mathrm{B}}\right)$, where B denotes here the effective subband size as allocated to the cell, $\mathrm{P_r}$ is the received useful signal power, Z stands for the cumulative interference power

in the allocated subband, and σ^2 is the thermal noise power density, set to -174 dBm/Hz. When not differently specified, we set $\mathrm{R_{th}}$= 40 Mbps.

Results are generated upon 600000 random deployments. Given the 18 cells, this results in above 10 million samples. By using the normal approximation of the binomial proportion for confidence interval estimation [14], it can be shown that this gives an above 95% confidence level in the estimate of the 0.001%-ile, within a $\pm$20% interval. Greedy coloring with vertex ordering is used for both the first graph and the subgraphs coloring in the second phase. In the simulations, greedy coloring applied to our deployments resulted in $\mathrm{M}+1$ colors in above $\sim$80% of the occurrences, and never exceeded $\mathrm{M}+2$. Same behavior applies for the coloring of the subgraphs in the second phase.

Figure 3 shows the empirical cumulative distribution function (ECDF) of the achievable data rates for the single phase graph construction with the M-neighbor criterion. The $\mathrm{M}=0$ case refers to the case in which no graph is constructed, i.e. all the cells are operating over the entire bandwidth. The curves in Figure 3(a) exhibit the typical behavior of spectrum reuse techniques in dense deployments. The usage of a low M in the graph construction, leads to an aggressive spectrum reuse which is beneficial for the cells that are not affected by significant interference and are therefore achieving very high rates (e.g., at the 90%-ile and above); however, it severely impact the cells which are strongly interference limited (below 10%-ile). Constructing the graph with a higher M improves instead the rates at the lower tail of the distribution, while penalizing the upper tail. Figure 3(b) highlights the behavior of the survival rates. At least a graph constructed with $\mathrm{M}=3$ is needed for supporting survival rates of e.g., above 2 Mbps.

The benefit of the proposed selective subgraph construction procedure is displayed in Figure 4, where the survival rates are shown as a function of the average data rate in the cell. As mentioned in section III, M' denotes the maximum number of neighbors used for constructing the subgraphs identified at the second phase. $\mathrm{M}'=0$ stands for the case where the second phase does not take place, and therefore the combination $\mathrm{M}=0,\mathrm{M}'=0$ denotes the case where the entire bandwidth is allocated to all the cells. As a general expected trend, survival data rates decrease with the configuration offering higher average rates. The proposed procedure leads to a significant improvement of the survival data rates, with a negligible impact on the average rates. All the gain is obtained by using a $\mathrm{M}'=1$ neighbor graph construction in the second phase. The usage of selective subgraph construction translates then to significant improvement of the network performance. For example, a survival rate of 2 Mbps can be obtained with our procedure by setting $\mathrm{M}=1,\mathrm{M}'=1$, while in a single phase graph construction $\mathrm{M}=3$ is needed; as a consequence, an average throughput of above $\sim$195 Mbps can be achieved with respect to the $\sim$155 Mbps of the single phase configuration with $\mathrm{M}=3$.

An overview of the achievable rates is presented in Table I, where the 50%-ile and 5%-ile rates are also included. The

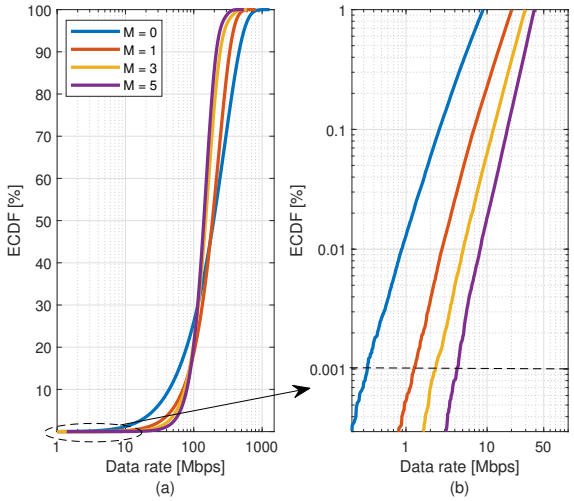

Fig. 3. ECDF of the achievable rates in a single stage graph construction (a), with highlight on the survival rates (b).

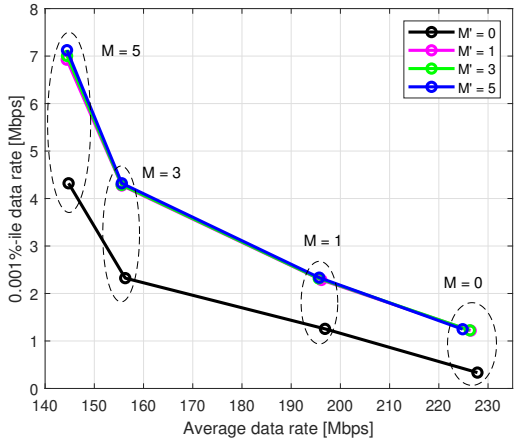

Fig. 4. Survival rates as a function of the average cell rate for the different subgraph construction configurations.

percentage gain for survival rates with respect to single phase graph construction is highlighted. The activation rate $\mathrm{A_r}$ in the last column refers to the percentage of deployments for which the subgraph construction procedure is activated, depending on whether cells unable to satisfy the rate threshold condition appear after the first phase. As expected, such activation rate decreases as M increases; when the number of subbands allocated in the first phase becomes larger, the number of cells requiring further orthogonalization diminishes indeed. Subgraph construction always offer significant relative gains in terms of survival rates, with a negligible or minor impact in terms of median and outage rates. Note that for $\mathrm{M}=0$, the subgraph construction has also a relevant benefit for the 5%-ile rates, while elsewhere such rates are not negatively impacted.

A sensitivity analysis to the selection of the data rate threshold $\mathrm{R_{th}}$ for activation of second phase graph construction, is presented in Figure 5, where both survival rate and 5%-ile

TABLE I
ACHIEVABLE RATES [MBPS] FOR
DIFFERENT SUBGRAPH CONSTRUCTION CONFIGURATIONS

	Average	50%-ile	5%-ile	0.001%-ile	A_r
M=0	227.84	195.12	25.76	0.33	-
M=0, M'=1	229.48	195.62	41.66	1.22 (+270%)	82.1%
M=0, M'=3	226.30	188.96	40.81	1.23 (+273%)	82.1%
M=0, M'=5	224.84	186.89	39.25	1.25 (+278%)	82.1%
M=1	196.87	187.25	47.25	1.26	-
M=1, M'=1	196.12	185.27	50.07	2.29 (+82%)	49.3%
M=1, M'=3	195.60	184.92	49.46	2.32 (+84%)	49.3%
M=1, M'=5	195.70	185.09	49.34	2.33 (+85%)	49.3%
M=3	156.28	148.97	56.03	2.32	-
M=3, M'=1	155.58	147.97	55.85	4.27 (+84%)	31.8%
M=3, M'=3	155.56	148.03	55.71	4.28 (+84%)	31.8%
M=3, M'=5	155.58	147.98	55.81	4.32 (+86%)	31.8%
M=5	144.77	140.15	63.70	4.28	-
M=5, M'=1	144.40	139.71	63.17	6.92 (+62%)	17.7%
M=5, M'=3	144.46	139.73	63.17	7.08 (+65%)	17.7%
M=5, M'=5	144.45	139.78	63.21	7.10 (+66%)	17.7%

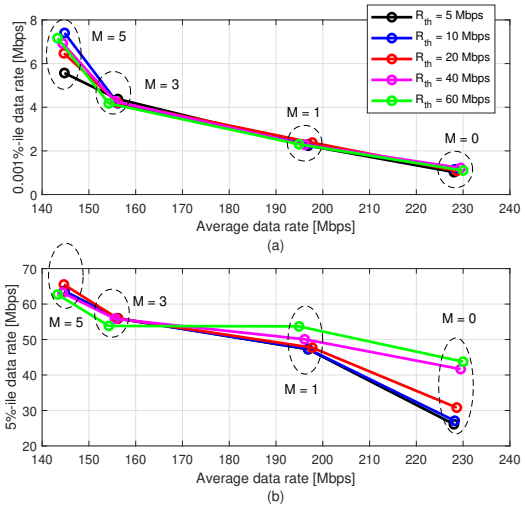

Fig. 5. Sensitivity of survival rates (a) and 5%-ile rates (b) to the selection of the second phase activation threshold $\mathrm{R_{th}}$, assuming $\mathrm{M'} = 1$.

rates are shown as a function of the average data rate. Only results obtained with $\mathrm{M'} = 1$ are shown. Survival rates appears to be weakly dependent to the selection of the threshold, with minor variations only appearing in the case of a high number of colors used in the first phase ($\mathrm{M} = 5$). Conversely, the 5%-ile rates are lower when the first phase construction does not take place ($\mathrm{M} = 0$) and a small $\mathrm{R_{th}}$ is used. This is because $\mathrm{R_{th}}$ is in such cases significantly lower than the achievable 5%-ile rates for single phase graph construction, therefore inhibiting potential gains from the second phase. No significant differences are instead visible when the number of colors in the first phase increase. As a rule of thumb, the threshold $\mathrm{R_{th}}$ should then be set to be significantly larger than the targeted 0.001%-ile rates, in order not to compromise potential gains also for the 5%-ile rates. In practice, such threshold is very dependent on the deployment and environment characteristics, and we foresee the usage of machine learning solutions for classifying such characteristics and mapping them to the threshold selection.

V. CONCLUSIONS AND FUTURE WORK

In this paper, we have proposed a novel centralized spectrum assignment technique for dense industrial wireless cells based on interference-aware selective subgraph construction. The scheme has been evaluated via extensive numerical simulations and shown to offer in a range of $\sim$70% to above $\sim$250% improvement in terms of survival rates (calculated at the 0.001%-ile of the distribution) with respect to a typical single phase graph construction. Gains are obtained by using a limited number of colors in the second phase. Such benefits come with negligible impact to median/average cell data rates, therefore improving the overall network performance.

Future work will study the performance of the proposed solutions considering dynamic environments, mobile radio cells and practical constraints in terms of estimation of interference matrix and signaling for centralized control. Also, machine learning approaches for the selection of the data rate threshold triggering the execution of the subgraph construction will be investigated.

REFERENCES

[1] R. Adeogun, G. Berardinelli, P. E. Mogensen, I. Rodriguez, and M. Razzaghpour, "Towards 6G in-X subnetworks with sub-millisecond communication cycles and extreme reliability," *IEEE Access*, vol. 8, pp. 110 172–110 188, 2020.

[2] D. Lopez-Perez, A. Valcarce, G. De La Roche, and J. Zhang, "OFDMA femtocells: A roadmap on interference avoidance," *IEEE communications magazine*, vol. 47, no. 9, pp. 41–48, 2009.

[3] K. N. Sivarajan, R. J. McEliece, and J. W. Ketchum, "Channel assignment in cellular radio," in *IEEE 39th Vehicular Technology Conference*. IEEE, 1989, pp. 846–850.

[4] B. Balasundaram and S. Butenko, "Graph domination, coloring and cliques in telecommunications," in *Handbook of optimization in telecommunications*. Springer, 2006, pp. 865–890.

[5] L. Narayanan, "Channel assignment and graph multicoloring," *Handbook of wireless networks and mobile computing*, vol. 8, pp. 71–94, 2002.

[6] L. Tan, Z. Feng, W. Li, Z. Jing, and T. A. Gulliver, "Graph coloring based spectrum allocation for femtocell downlink interference mitigation," in *2011 IEEE Wireless Communications and Networking Conference*. IEEE, 2011, pp. 1248–1252.

[7] M. Necker and M. C. Necker, "A graph-based scheme for distributed interference coordination in cellular OFDMA networks," in *VTC Spring 2008-IEEE Vehicular Technology Conference*. IEEE, 2008, pp. 713–718.

[8] F. Ahmed, O. Tirkkonen, M. Peltomäki, J.-M. Koljonen, C.-H. Yu, and M. Alava, "Distributed graph coloring for self-organization in LTE networks," *Journal of Electrical and Computer Engineering*, vol. 2010, 2010.

[9] T. D. Novlan, R. K. Ganti, A. Ghosh, and J. G. Andrews, "Analytical evaluation of fractional frequency reuse for OFDMA cellular networks," *IEEE Transactions on wireless communications*, vol. 10, no. 12, pp. 4294–4305, 2011.

[10] J. L. Gross and J. Yellen, *Graph theory and its applications*. CRC press, 2005.

[11] L. G. U. Garcia, K. I. Pedersen, and P. E. Mogensen, "Voice-Centric LTE Femtocells and Improper Graph Colorings," in *2012 IEEE 75th Vehicular Technology Conference (VTC Spring)*. IEEE, 2012, pp. 1–5.

[12] R. Adeogun, G. Berardinelli, I. Rodriguez, and P. Mogensen, "Distributed Dynamic Channel Allocation in 6G in-X Subnetworks for Industrial Automation," in *2020 IEEE Globecom Workshops (GC Wkshps*. IEEE, 2020, pp. 1–6.

[13] "Study on channel model for frequencies from 0.5 to 100 GHz (Release 16)," 3rd Generation Partnership Project, Tech. Rep. 38.901, 2019.

[14] L. D. Brown, T. T. Cai, A. Dasgupta *et al.*, "Confidence intervals for a binomial proportion and asymptotic expansions," *The Annals of Statistics*, vol. 30, no. 1, pp. 160–201, 2002.